Beam Test Results of a FPGA Prototype of a Front-end Trigger Device for CMS Muon Barrel Chambers

M. De Giorgi[1], A. De Min[1], I. Lippi[1], R. Martinelli[1], A. J. Ponte Sancho[1] and P. Zotto[2]

Dipartimento di Fisica dell'Università di Padova e Sezione dell'I.N.F.N. di Padova, Italy
Dipartimento di Fisica del Politecnico di Milano e Sezione dell'I.N.F.N. di Padova, Italy

1. Introduction

The triggering front-end device foreseen in the CMS muon barrel chambers is the Bunch and Track Identifier (BTI).

The BTI, in its basic version, triggers at the alignment of all the hits in the group of drift tubes interested by the muon. The coincidence of these hits happens at fixed time after the muon traversed the array of drift tubes and the BTI can extract the full track information (slope and intercept). The complete description of the mechanism and the conceptual design of a fully working device is available in [1].

Although the device can reasonably be realized only with an ASIC, it can be partially implemented using FPGA technology. The analysis of the performance is anyway useful in giving indications for the design of the full custom version.

Three FPGA prototypes of BTI were produced in 1995 and tested on a muon beam during summer 1995 and spring 1996. The results of the test are summarized in this paper.

2. Design of the Prototype

A prototype realized using FPGA is obviously limited by the available size and speed of the ICs. The implementation of the algorithm encountered serious space limitations, forcing to downgrade the requirements.

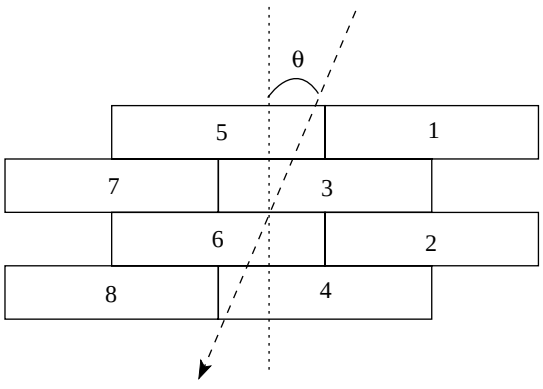

Figure 1 - FPGA prototype BTI allocation.

The actual gate array used was XILINX XC4013, 6 ns grade.

The BTI prototype was thought as a device programmable for fixed incidence angle, as it is always the case in the test beam setup. In this case the BTI generates a valid trigger signal when the track is in the programmed angular range and hence there is no need for an evaluation of the track slope as in the full design. Due to space limitations, no information on position is output from the BTI.

The number of wires, allocated to the prototype as in Figure 1, is 8, instead of 9 as was later foreseen for the complete BTI, and only a subgroup of relevant couples of wires was considered.

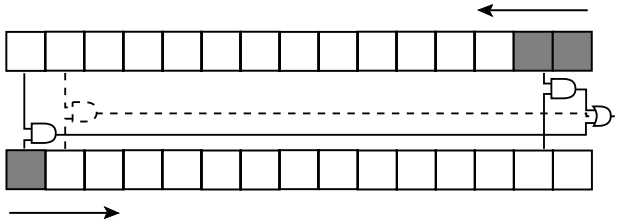

Figure 2 - Shift register of a couple of wires showing acceptance. The input position of the upper shift registers is programmable as a function of the track inclination.

As shown in Figure 2, the signals coming from each couple of wires are shifted in opposite directions inside a pair of shift registers whose depth is programmable as a function of the maximum drift-time T_{MAX}. The shifting frequency is 40 MHz (compared to 80 MHz of the final VLSI circuit): therefore the shift of one cell corresponds to 25 ns.

At every clock step the AND of the two vertically aligned bits of the shift registers is evaluated. The tolerance allowed in the AND evaluation is built in from the fact that the signal running in the upper shift register is two cells wide, while the signal inside the lower one is only one cell wide. This choice is a compromise between efficiency and noise of the device.

The programmability for fixed angles means that, depending on the chosen angular range and the actual drift

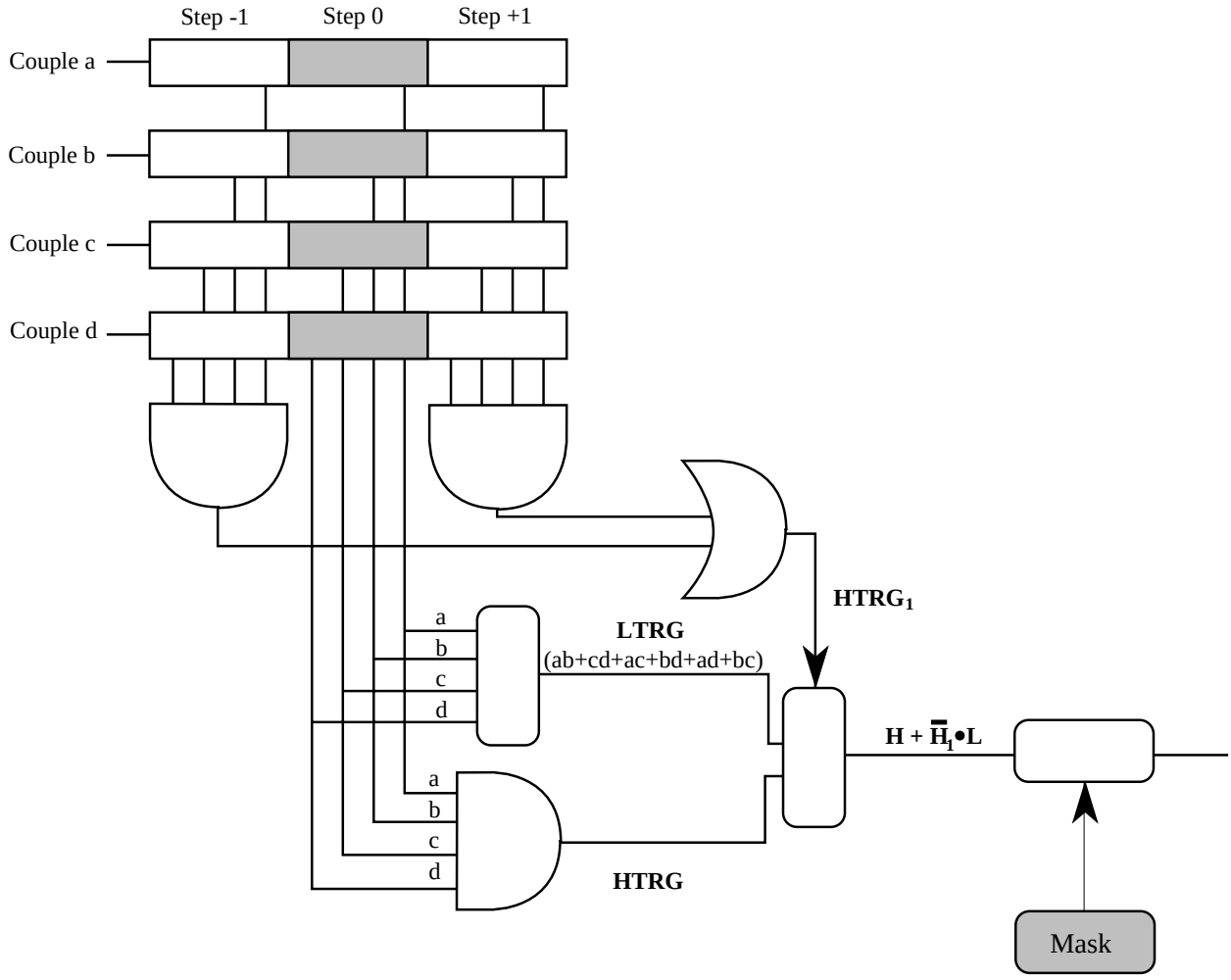

Figure 3 - Block diagram of the logic of one of the fifteen patterns implemented in the BTI prototype.

velocity, for each wire couple the signals are input to a programmed depth inside the upper shift register and the coincidence is output with a predefined delay, chosen to synchronize each couple. A look-up table, including an initial shift and a delay for each couple, is loaded for each angular configuration.

The couples are grouped in patterns, each one including 3 or 4 couples, whose coincidence is evaluated at every clock cycle. Inside each pattern only the couples with the electron drift in opposite directions are considered. If any two of the couples of the pattern give a coincidence signal a Low Level Trigger (LTRG) is generated, while a High Level Trigger (HTRG) is generated if a signal from all the couples of the pattern is available. The information about the triggering pattern and the trigger type is not recorded.

A noise reduction mechanism is available, because the LTRG signal is issued only if at the neighbouring steps there is no HTRG generated. A block diagram of the device logic, showing all the previously explained features, is given in Figure 3.

3. Test Setup

A drift chamber prototype [2], with four layers of 16 drift tubes each, was equipped with three FPGA BTI prototypes staggered by one cell as in the final design. They were tested in the CERN H2 muon beam with a free running clock.

The BTI is a synchronous device and therefore its performance is strictly correlated to the synchronization. The recorded TDC data included drift times, BTI generated trigger signals and the BTI clock to allow the computation of the phase of each event for the BTI with respect to the test beam experiment trigger.

The data were recorded using 2277 Lecroy TDCs, with 1 ns least count and multihit capability, and the XILINX cards were put after 60m long cables: the difference in delay between signals on different wires introduced by the

line length was measured with testpulses and was found within ±4ns.

Data were taken at several inclinations of the wires with respect to the beam and at several magnetic field values.

The BTI was programmed for a maximum drift-time T_{MAX} = 350 ns. This programmation was never changed, even when the magnetic field was switched on modifying the apparent drift velocity.

4. Results

The major task of the test was the evaluation of the efficiency of the triggering mechanism, being all the other interesting checks ruled out by space limitations in the FPGA implementation of the BTI.

The efficiency is defined as the fraction of events giving a BTI trigger at the expected time with respect to the particle crossing (in our setup the 23rd clock step).

4.1 Efficiency versus Synchronization

The data were taken asynchronously and therefore the first important check was done on the performance of the BTI as a function of the phase with respect to particle crossing, since we expect that events are assigned the wrong crossing when the phase is lost. The efficiency of the device as a function of the synchronization time is shown in Figure 4 for a sample of data at $\theta = 0^0$ and B = 0T. The efficiency exhibits an almost flat top at ±5ns from the central value and drops when the BTI clock is too early or too late. Events in the range of ±5ns from the central value are in the following called synchronous events. A more detailed analysis of the data shows that the missing fraction of events is assigned to the step before the expected one if the clock is too early and to the step after the expected one if the clock is too late. The result is confirmed from a simulation of the device using only synchronous data outphased by the wanted time.

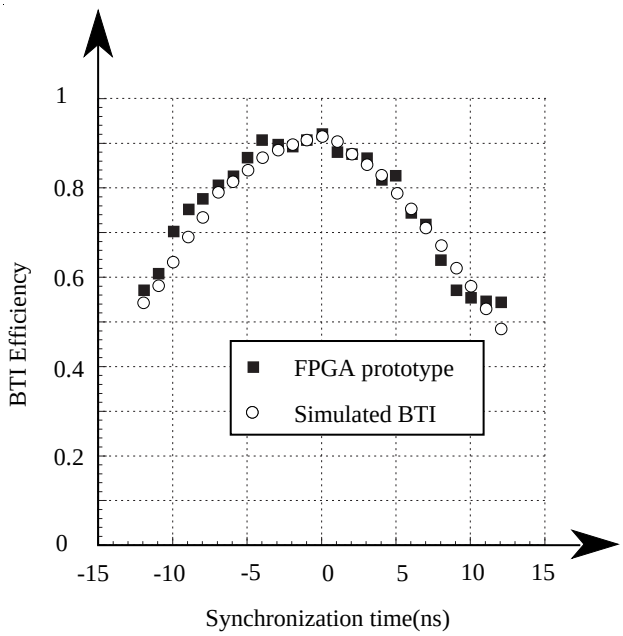

Figure 4 - BTI efficiency vs synchronization with the experiment trigger.

4.2 Efficiency versus drift time

The BTI was programmed for a maximum drift-time T_{MAX} = 350 ns, but the actual maximum drift time can be different. We have recorded data where the maximum drift-time was T_{MAX} = 335ns. The effect on the performance of the bad matching between expected and actual value can be seen in Figure 5, where the efficiency versus the drift time of the wire in the first layer shows a seesaw behaviour with a 25 ns period. This means that close to certain drift-times the device sampling assigns the input signal to the wrong step, and the tight coincidence allowed for the signals is not verified anymore.

This effect should not cause an inefficiency in the full device, but rather a slightly different slope computation.

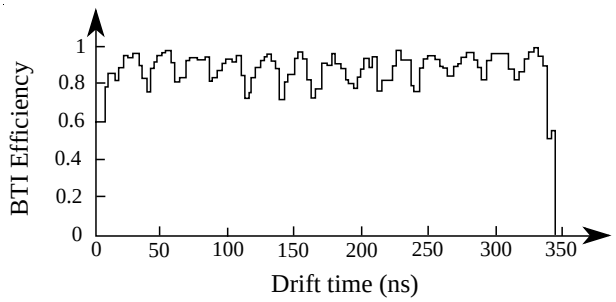

Figure 5 - BTI efficiency as a function of the drift time of the wire in the first layer for θ = 0 sample.

4.3 Uniformity response of BTIs

The drift times associated to an event can be used to fit a straight line through the four layers. We reconstructed all the tracks with at least three points using a fit probability cut at 0.1 % and allowing the rejection of the worst measurement for the four points tracks. Then we measured the fraction of events with a reconstructed track in which there was a BTI signal at the expected step.

The request of a fitted track excludes two non negligible contributions to the overall inefficiency. Indeed it factorizes out the contribution of chamber inefficiency, since it excludes from counting the events in which the fit could not be performed due to missing drift times, and the contribution of cases of penetrating δ-rays or

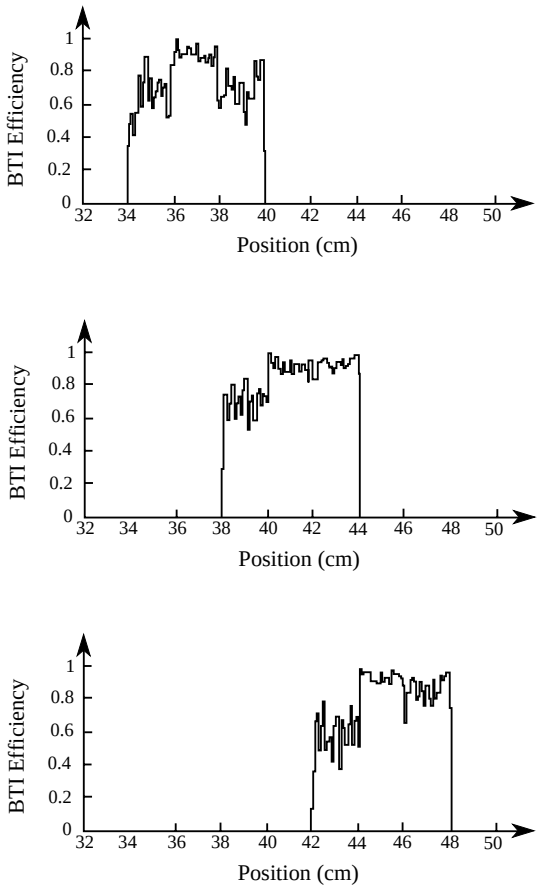

Figure 6 - Efficiency as a function of position for each BTI.

electromagnetic showers that spoiled the drift time measurement in more than one cell.

Therefore the prototype efficiency is affected only by the effect of soft δ-rays fully contained in a cell.

Data were collected using three BTI's. Each of them was covering 6 cm of the chamber, but they were staggered by 4 cm providing a 2 cm superposition between two consecutive devices. The total covered area of the chamber was therefore 14 cm wide.

It is possible to make a comparison of the performance of the three prototypes, looking at the efficiency in the respectively covered areas.

The efficiency of the prototypes is shown as a function of position in Figure 6. It can be immediately noticed that every prototype, as an effect of a choice in the design, has a lower efficiency in the first two centimeters covered. Infact since this range is meant to be covered from the previous BTI, not all the necessary couples were implemented. On the contrary each BTI was programmed to be fully efficient in the next four centimeters covered.

This is well verified for two of them, while there is an inefficiency in the first one, probably due to the PCB

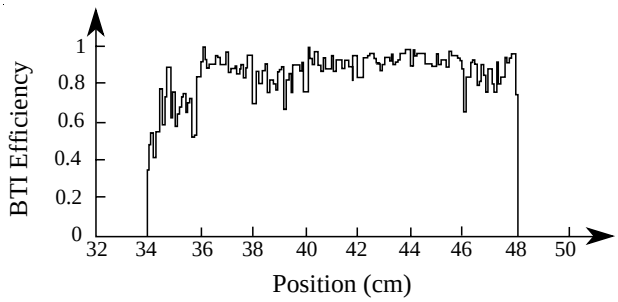

Figure 7 - BTI efficiency as a function of the position in the chamber frame.

layout. This inefficiency is anyway completely recovered from the superposition of the second one, owing to the existing redundancy, as we can see from Figure 7, where all the BTIs are plotted together.

4.4 Efficiency versus Track Inclination

The track fitting can also be used to investigate the efficiency of the BTI as a function of the incidence angle. The angular acceptance of each couple is quite different. Therefore the full efficiency of the device is expected to be found in a short angular range defined by the superposition of the acceptances of each couple. Unfortunately this range becomes shorter for increasing track inclinations.

The effect of the uneven angular acceptance of the couples is clearly visible in Figure 8, where the BTI efficiency is plotted as a function of the fitted angle for two samples of data: the efficiency monotonically decreases as the angle becomes more negative and an efficiency reduction is clearly visible at angles greater than 11^0. These effects are easily explained by checking the

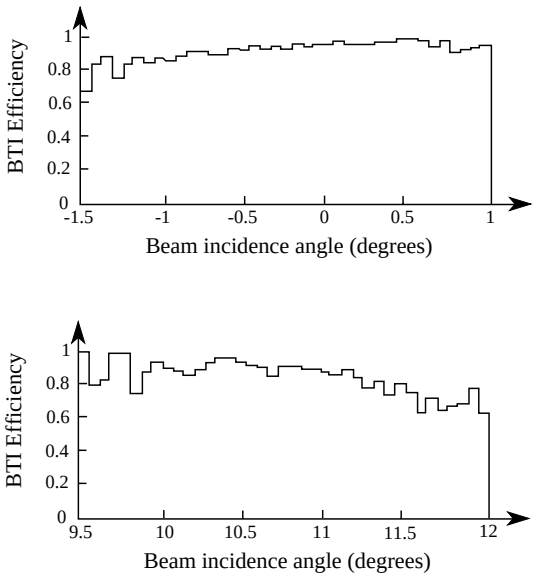

Figure 8 - BTI efficiency as a function of fitted angle.

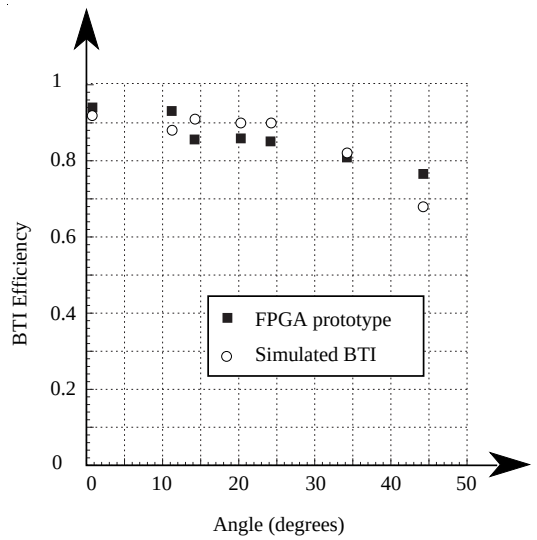

Figure 9 - Efficiency as a function of incident angle.

acceptance of each programmed configuration and the behaviour is well reproduced by the FPGA prototype BTI simulation.

The average efficiency in the fully covered geometrical range for synchronous events that can be extracted from the data is given in Figure 9. The efficiency is compared with the expectation results of the Montecarlo used to tune up the prototype design and to define the sets of couples, their delays and their initial shifts for every angular range. The reasonable agreement between the actual efficiency and the expected one is an indication of the good status of understanding of the performance of the drift tubes.

There is a large difference in the expected behaviour of the FPGA prototype and the designed full scale device. The latter is expected to have efficiencies better than the ones quoted, since there is no angular acceptance cut in its design.

4.5 Efficiency in Magnetic Field

Data were taken in magnetic field in the situation shown in Figure 10 with the chamber inclined at $\theta = 20^0$. This configuration will be existing in CMS only in the longitudinal view, which is less important for the trigger, but it is one of the worst possible situations.

B(T)	T_{MAX}(ns)	V_d(μm/ns)	Efficiency
0.0	335	59.7	85.9%
0.5	345	58.0	80.7%
1.0	375	53.3	11.4%
1.5	420	47.6	0.1%

Table 1 - Apparent drift velocity modification and BTI efficiency as a function of magnetic field for $\theta = 20^0$.

The effect of a magnetic field perpendicular to the wire direction is an elongation of the drift path of the electrons to the anode, resulting in a longer maximum drift time and therefore in an apparent modification of the drift velocity. These apparent changes and the efficiency are reported in Table 1. Instead the other magnetic field component introduces deviations from linearity of the space-time relationship.

Apparently the device is not very much sensitive to fields as high as B = 0.5T even without changing its default programmation. Of course the drop in efficiency at higher fields can be recovered at least partially, as long as distorsions are limited, programming the BTI for the actual apparent drift velocity inside the field.

Further studies are planned to have a real understanding of the performance of the device with the chamber in the magnetic field.

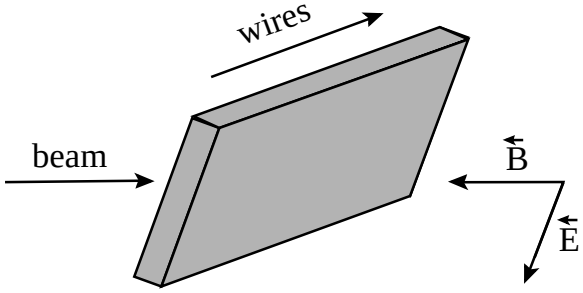

Figure 10 - Relative directions of beam, chamber, electric and magnetic fields in the test beam setup.

6. Conclusions

The beam test of the fixed angle prototype version of the BTI, realized in FPGA, was satisfactory, since its performance fully agrees with expectations. Once all the effects of the design limitations are considered, the efficiency of the device was very close to the geometrical efficiency.

The result of the detailed analisys confirms the validity of the design choices and is completely coherent with all the previously performed computations.

References

[1] M. De Giorgi et al, *Proceedings of the First Workshop on Electronics for LHC experiments*, 222-227.

[2] A. Benvenuti et al, *"Performance of the Drift Tubes for the Barrel Muon Chambers of the CMS Detector at LHC"*, in preparation.